Journal of Advanced Ceramics
2017, **6**(1): 50–58
DOI: 10.1007/s40145-016-0217-x

ISSN 2226-4108
CN 10-1154/TQ

Research Article

Microstructures and microwave dielectric properties of $(Ba_{1-x}Sr_x)_4(Sm_{0.4}Nd_{0.6})_{28/3}Ti_{18}O_{54}$ solid solutions

Xianpei HUANG[a], Xinyu LIU[a], Fei LIU[b,*], Changlai YUAN[a,c], Jingjing QU[d], Jiwen XU[a], Changrong ZHOU[a], Guohua CHEN[a]

[a]*School of Material Science and Engineering, Guilin University of Electronic Technology, Guilin 541004, China*
[b]*School of Mechanical and Electrical Engineering, Guilin University of Electronic Technology, Guilin 541004, China*
[c]*Guangxi Key Laboratory of Information Materials, Guilin University of Electronic Technology, Guilin 541004, China*
[d]*Department of Information Engineering, Guilin University of Aerospace Technology, Guilin 541004, China*

Received: October 17, 2016; Revised: December 01, 2016; Accepted: December 19, 2016

Abstract: $(Ba_{1-x}Sr_x)_4(Sm_{0.4}Nd_{0.6})_{28/3}Ti_{18}O_{54}$ ($x = 0.02$, 0.04, 0.06, 0.08, 0.1) solid solutions were prepared by the conventional solid-state reaction process. It was found that $(Ba_{1-x}Sr_x)_4(Sm_{0.4}Nd_{0.6})_{28/3}Ti_{18}O_{54}$ ceramics are fully composed of $BaSm_2Ti_4O_{12}$ and $BaNd_2Ti_5O_{14}$ phases for all the compositions. The increasing x value ($0.02 \leqslant x \leqslant 0.1$) in $(Ba_{1-x}Sr_x)_4(Sm_{0.4}Nd_{0.6})_{28/3}Ti_{18}O_{54}$ ceramics can not only obtain high $Q \times f$ value but also effectively enhance the permittivity (ε_r). The $(Ba_{1-x}Sr_x)_4(Sm_{0.4}Nd_{0.6})_{28/3}Ti_{18}O_{54}$ ceramic with $x = 0.08$, sintered at 1440 ℃ for 4 h, shows excellent microwave dielectric properties of permittivity (ε_r) ≈ 93.19, quality factor ($Q \times f$) ≈ 9770.14 GHz (at 3.415 GHz), and almost near-zero temperature coefficient of resonant frequency (τ_f) ≈ +4.56 ppm/℃.

Keywords: tungsten bronze type; high permittivity; microwave dielectric properties

1 Introduction

As is well-known, the microwave dielectric ceramic materials with high quality factor ($Q \times f$) and high permittivity (ε_r) have been developed for applications in satellite positioning, navigation, and wireless communication. At present, microwave telecommunication and satellite broadcasting has become one of the fastest developing segments in the communications and electronics industry. Meanwhile, the widespread usage of several wireless systems has required dielectric components that are low-cost, lightweight, small, multifunctional, and highly reliable to reduce the device size. In addition, high dielectric constant, high quality factor, and near-zero temperature coefficient of resonant frequency are three key properties required for microwave resonator materials [1].

In early time, Bolton [2] has reported one unknown $BaO–Nd_2O_3–TiO_2$ ternary compound, which has a high relative permittivity (ε_r) and a low temperature coefficient of resonant frequency (τ_f). Later, Ohsato and co-workers [3,4] have done extensive work on the preparation, characterization, and structure and property investigation of tungsten bronze type materials. In addition, Valant *et al*. [5] and Varfolomeeva and Miranov [6] displayed $Ba_{3.75}Nd_{9.5}Ti_{18}O_{54}$ and $BaNd_2Ti_4O_{12}$ compounds as specific compositions of the solid solution phase $Ba_{6-3x}Nd_{8+2x}Ti_{18}O_{54}$ ($0 \leqslant$

* Corresponding author.
E-mail: liufeiguet@yahoo.com

$x \leqslant 0.75$). According to several authors [7,8], $Ba_{6-3x}Ln_{8+2x}Ti_{18}O_{54}$ ceramics based on Gd, Sm, and Nd have high quality factors ($Q \times f$) up to 14,000 GHz, and the La-based ceramics have the highest relative permittivity ($\varepsilon_r = 104$). Ohsato *et al.* [9] have also established a relation between the microwave dielectric properties of $Ba_{6-3x}Sm_{8+2x}Ti_{18}O_{54}$ ($0.3 \leqslant x \leqslant 0.7$) solid solution and the crystal structure. It shows that substitution of Sm^{3+} for Ba^{2+} in the large cation sites results in the creation of vacancies and crystal distortion, indicating that the shrinkage of the TiO_6 octahedral site plays an important role for the improvement of microwave dielectric properties.

The microwave dielectric properties of $Ba_{6-3x}Ln_{8+2x}Ti_{18}O_{54}$ (Ln = La, Nd, Sm) materials have been studied sufficiently due to their high permittivity. However, the restriction of $Q \times f$ and τ_f values impedes their commercial application [10–13]. Furthermore, there are a large number of active atoms at the solid solution surface, which has a high interfacial dielectric loss induced by interface polarization [14,15]. In order to resolve these problems, much work has been done to improve the $Q \times f$ and τ_f values. Many attentions have been paid to improve the microwave dielectric properties by substitution of Ba^{2+} and Nd^{3+} ions using Sr^{2+} and Y^{3+} ions, as well as adding $NdAlO_3$ or Al_2O_3. As can be seen from Table 1, all of them find that the substitution of ions can significantly enhance $Q \times f$ and reduce τ_f [16–19].

$Ba_{6-3x}Ln_{8+2x}Ti_{18}O_{54}$ (Ln = La, Nd, Sm) has been reported to possess high permittivity (ε_r) and quality factor ($Q \times f$) [20–24]. The aim of our present work is to improve the microwave dielectric properties of $(Ba_{1-x}Sr_x)_4(Sm_{0.4}Nd_{0.6})_{28/3}Ti_{18}O_{54}$ by substituting the Sr^{2+} ions. The effects of substitution of Sr^{2+} ions on the microstructures and microwave dielectric properties of $(Ba_{1-x}Sr_x)_4(Sm_{0.4}Nd_{0.6})_{28/3}Ti_{18}O_{54}$ ceramics are investigated systematically.

Table 1 Dielectric properties of $Ba_{6-3x}Ln_{8+2x}Ti_{18}O_{54}$ ceramics

Traditional sample	ε_r	$Q \times f$ (GHz)	τ_f (ppm/℃)
$Ba_{6-3x}(Sm_{0.2}Nd_{0.8})_{8+2x}Ti_{18}O_{54}$ (x = 2/3)	80.80	8100	+35.5
$Ba_{6-3x}(Sm_{0.9}Bi_{0.1})_{8+2x}Ti_{18}O_{54}$ (x = 2/3)	84.10	7840	–21.0
$(Ba_{1-x}Sr_x)_{4.2}Sm_{9.2}Ti_{18}O_{54}$ (x = 0.04)	80.60	9590	–11.9
$(Ba_{0.6}Pb_{0.4})_{6-3x}La_{8+2x}Ti_{18}O_{54}$ (x = 1.5)	95.00	6000	+200.0
$Ba_{6-3x}(Sm_{0.9}La_{0.1})_{8+2x}Ti_{18}O_{54}$ (x = 2/3)	84.00	9000	+4.2
$(Ba_{0.8}Sr_{0.2})_{6-3x}Nd_{8+2x}Ti_{18}O_{54}$ (x = 0.2)	95.00	5500	+125.0
$(Ba_{0.7}Sr_{0.3})_{4.8}(Sm_{0.7}La_{0.3})_{8.8}Ti_{18}O_{54}$	98.77	5184	+10.9

2 Experimental procedure

The raw materials were high-purity oxide powders: $BaCO_3$ (99.8%, Guo-Yao Co. Ltd., Shanghai, China), $SrCO_3$ (99.8%, Guo-Yao Co. Ltd., Shanghai, China), Nd_2O_3 (99.8%, Guo-Yao Co. Ltd., Shanghai, China), Sm_2O_3 (99.8%, Guo-Yao Co. Ltd., Shanghai, China), and TiO_2 (99%, Guo-Yao Co. Ltd., Shanghai, China), and they were mixed according to the desired stoichiometry $(Ba_{1-x}Sr_x)_4(Sm_{0.4}Nd_{0.6})_{28/3}Ti_{18}O_{54}$ (x = 0.02, 0.04, 0.06, 0.08, 0.1). The mixed powders were ground in distilled water for 24 h in a ball mill with ZrO_2 balls, then dried and calcined at 1100 ℃ for 4 h in air. The calcined powders were ground into fine powders, and then the fine powders were pressed into pellets with dimensions of 12 mm in diameter and 5–6 mm in thickness under a pressure of 150 MPa, with 5 wt% PVA as binder. These pellets were sintered at temperatures of 1400–1460 ℃ for 4 h in air.

The apparent density (ρ_a) of sintered ceramics was measured by the Archimedes method, and the bulk density (ρ_b) was evaluated from the dimensions and weight. Correspondingly, the relative density (ρ_r) was calculated with the following formula:

$$\rho_r = \frac{\rho_a}{\rho_b} \times 100\% \quad (1)$$

The crystalline phases of the sintered ceramics were identified by X-ray diffraction (XRD) using Cu Kα radiation (Rigaku D/MAX-2400 X-ray diffractometer, Tokyo, Japan). Surface topologies of the ceramics were observed by scanning electron microscopy (SEM; JSM-6460, JEOL, Tokyo, Japan). Meanwhile, in order to investigate the effect of Sr^{2+} substitution for Ba^{2+}, the $(Ba_{1-x}Sr_x)_4(Sm_{0.4}Nd_{0.6})_{28/3}Ti_{18}O_{54}$ (x = 0.08) ceramic was studied by energy-dispersive X-ray spectroscopy (EDX). Microwave dielectric properties of the ceramics were measured by the $TE_{01\delta}$ shielded cavity method with a network analyzer (8720ES, Agilent, Palo Alto, CA, USA) and a temperature chamber (Delta9023, Delta Design, Poway, CA, USA) in the temperature range of 25–75 ℃ [25,26]. The temperature coefficient of resonant frequency (τ_f) value was calculated with the following formula [27]:

$$\tau_f = \frac{\Delta f_0}{f_0 \Delta T} = \frac{f_{75} - f_{25}}{f_{25} \times 50} \quad (2)$$

where f_{25} and f_{75} were the resonant frequencies at 25 ℃ and 75 ℃, respectively.

3 Results and discussion

3.1 Crystalline structures

Figure 1(a) illustrates the room-temperature XRD patterns recorded from $(Ba_{1-x}Sr_x)_4(Sm_{0.4}Nd_{0.6})_{28/3}Ti_{18}O_{54}$ ($x=0.02$, 0.04, 0.06, 0.08, 0.1) ceramics sintered at 1440 ℃ for 4 h. As shown in Fig. 1(a), Bragg peaks corresponding to the tungsten bronze-like crystal structure are observed in the ceramics. And it can be indexed as a tungsten bronze structure with formulae $BaSm_2Ti_4O_{12}$ (JCPDS Card No. 44-0062) and $BaNd_2Ti_5O_{14}$ (JCPDS Card No. 33-0166), belonging to orthorhombic phase. All the samples doped with different amounts of Sr^{2+} ions have the same diffraction patterns. In the $Ba(A2)Nd_2(A1)Ti_5(B)O_{14}$ solid solution, there are three kinds of cations with different ionic radii in the crystal structure. The middle-sized Ln^{3+} ions mainly occupy A1 rhombic sites, the largest Ba^{2+} ions mainly occupy pentagonal A2 sites, and the smallest Ti^{4+} ions alone occupy octahedral B sites [28]. The A2 sites are occupied by four Ba^{2+} ions and A1 sites by eight Ln^{3+} ions. Therefore, the dielectric properties of the solid solutions are highly influenced by crystal structure. Substitution of Sr^{2+} ions (1.44 Å) for Ba^{2+} ions (1.61 Å) in the large cation sites (A2) results in the crystal distortion, showing that the shrinkage of the TiO_6 octahedral site plays an important role for improvement of the microwave dielectric properties. At the same time, the distortion of the crystal lattice of the $BaNd_2Ti_5O_{14}$ phase is also expected to influence the microwave dielectric properties of the produced ceramics, which is attributed to the presence of Sr^{2+} ions substituted for Ba^{2+} cations. As can be seen from Fig. 1(b), with increasing sintering temperature, $BaNd_2Ti_5O_{14}$ and $BaSm_2Ti_4O_{12}$ diffraction peaks are not obviously changed, and $BaNd_2Ti_5O_{14}$ diffraction peaks at the angles of 38°–40° are strengthened for the specimen sintered at 1440 ℃.

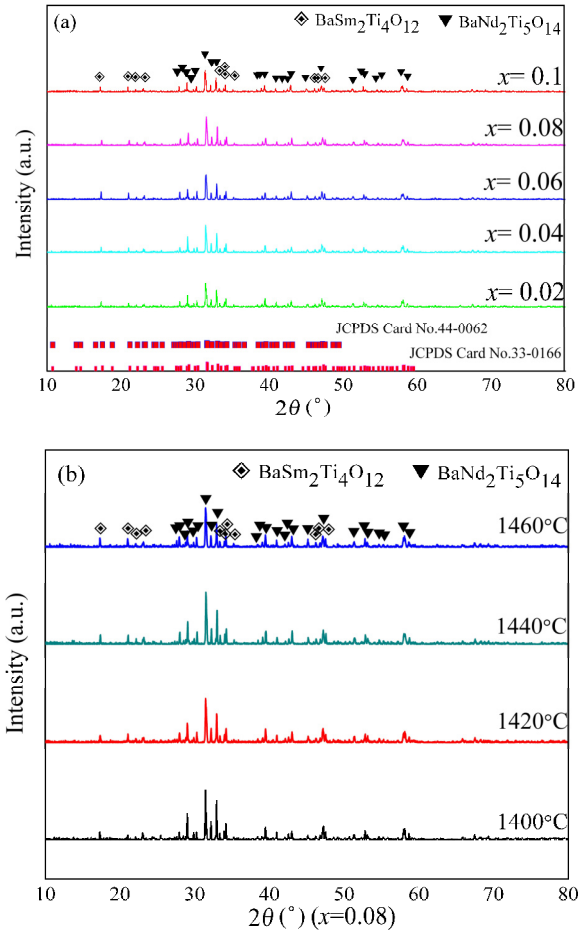

Fig. 1 XRD patterns of $(Ba_{1-x}Sr_x)_4(Sm_{0.4}Nd_{0.6})_{28/3}Ti_{18}O_{54}$ ceramic specimens: (a) $(Ba_{1-x}Sr_x)_4(Sm_{0.4}Nd_{0.6})_{28/3}Ti_{18}O_{54}$ ($x=0.02$, 0.04, 0.06, 0.08, 0.1) ceramics sintered at 1440 ℃ for 4 h; (b) $(Ba_{1-x}Sr_x)_4(Sm_{0.4}Nd_{0.6})_{28/3}Ti_{18}O_{54}$ ($x=0.08$) ceramic at different sintering temperatures.

3.2 Microstructures and density

Figure 2 shows the SEM micrographs of $(Ba_{1-x}Sr_x)_4(Sm_{0.4}Nd_{0.6})_{28/3}Ti_{18}O_{54}$ ceramics sintered at 1440 ℃ for 4 h. As can be found from the micrographs, all the samples show dense and homogeneous microstructures. Also, with the increase in the number of Sr^{2+} ions, the pores appear in the microstructures. At the same time, an excess of Sr^{2+} ions results in the agglomeration phenomena, preventing the better densification. On the other hand, EDX analysis was used by combining with SEM to prove that the substitution of Sr^{2+} for Ba^{2+} has been successfully executed, as shown in Fig. 3. It is obvious that the Sr^{2+} ions can substitute for Ba^{2+} ions, which is in agreement with the results of XRD patterns in Fig. 1(a). In addition, in order to understand how the Sr^{2+} ions affect the microstructures of $(Ba_{1-x}Sr_x)_4(Sm_{0.4}Nd_{0.6})_{28/3}Ti_{18}O_{54}$ ($0.02 \leqslant x \leqslant 0.1$) ceramics, cross-sectional SEM micrographs are taken as shown in Fig. 4. $(Ba_{1-x}Sr_x)_4(Sm_{0.4}Nd_{0.6})_{28/3}Ti_{18}O_{54}$ ($0.02 \leqslant x \leqslant 0.1$) ceramics show agglomeration and dense and homogeneous microstructures. Furthermore, it can be clearly seen that the porosity increases with increasing x value, implying that an increase of Sr^{2+} ions ($x \geqslant 0.1$) may deteriorate the densification of the specimens. From the observation of microstructure, the $Q \times f$ value is influenced by the defect, which results from that the

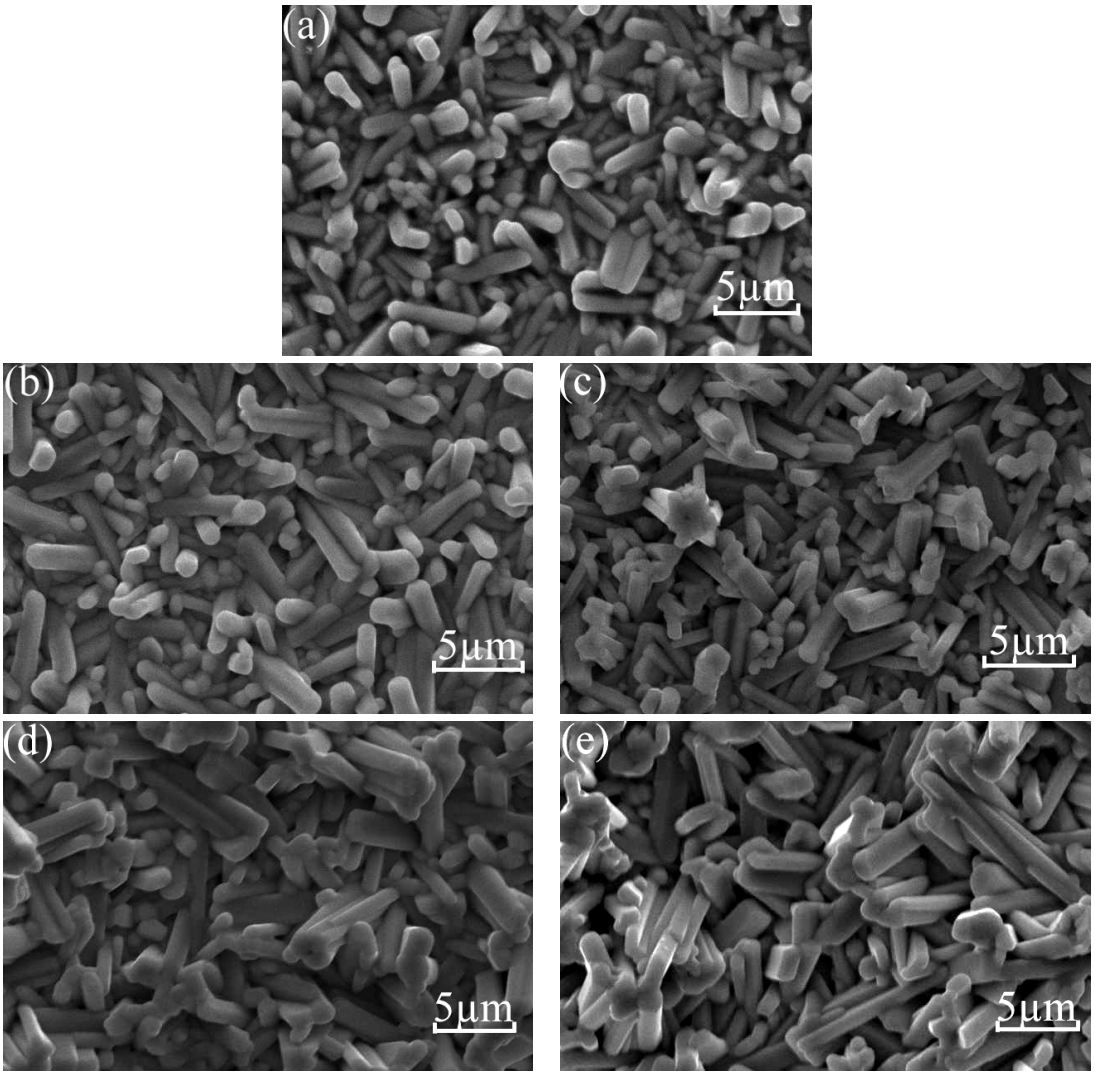

Fig. 2 SEM micrographs of $(Ba_{1-x}Sr_x)_4(Sm_{0.4}Nd_{0.6})_{28/3}Ti_{18}O_{54}$ ceramics with (a) $x = 0.02$, (b) $x = 0.04$, (c) $x = 0.06$, (d) $x = 0.08$, and (e) $x = 0.1$, sintered at 1440 ℃ for 4 h.

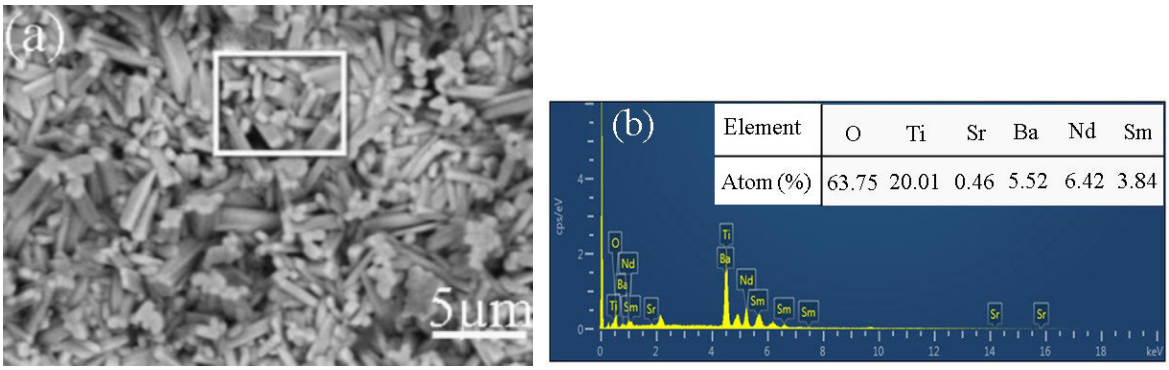

Fig. 3 EDX analysis of the $(Ba_{1-x}Sr_x)_4(Sm_{0.4}Nd_{0.6})_{28/3}Ti_{18}O_{54}$ ceramic ($x = 0.08$) sintered at 1440 ℃ for 4 h.

defect can reduce the compactness of sintered ceramics and cause a decrease in $Q \times f$ value. In addition, Fig. 5 shows the SEM images of the $(Ba_{1-x}Sr_x)_4(Sm_{0.4}Nd_{0.6})_{28/3}Ti_{18}O_{54}$ ceramic with $x = 0.08$ sintered at different temperatures. As seen in Fig. 5, for the composition with $x = 0.08$, the densification degree increases with the increasing sintering temperature from 1400 to 1440 ℃, and then decreases gradually when the sintering temperature is raised around 1460 ℃. This phenomenon means that the degree of

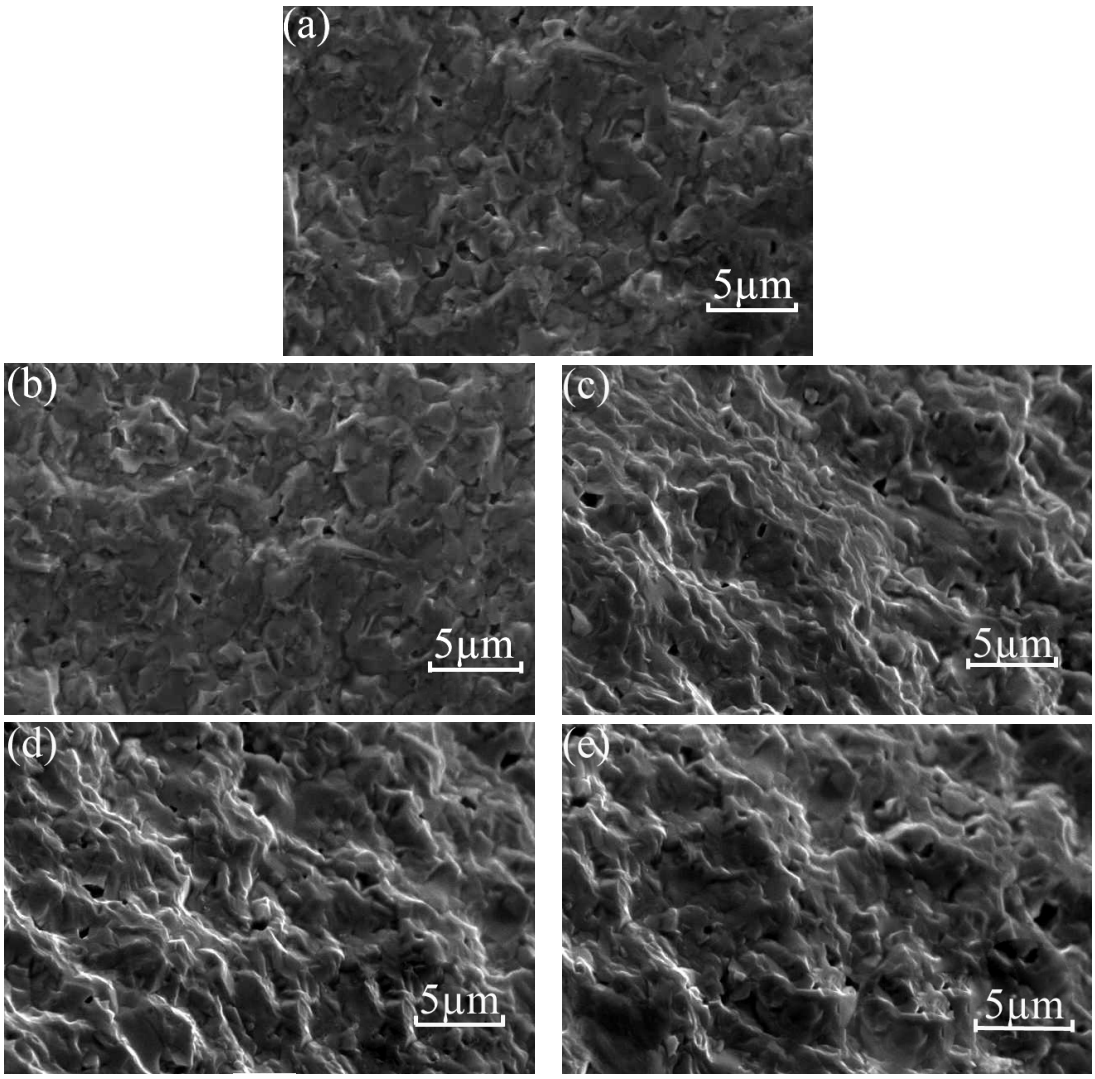

Fig. 4 SEM micrographs of the cross-section of $(Ba_{1-x}Sr_x)_4(Sm_{0.4}Nd_{0.6})_{28/3}Ti_{18}O_{54}$ ceramics with (a) $x = 0.02$, (b) $x = 0.04$, (c) $x = 0.06$, (d) $x = 0.08$, and (e) $x = 0.1$, sintered at 1440 ℃ for 4 h.

densification at 1440 ℃ is higher than that of other sintering temperatures.

In addition, Fig. 6(a) shows the apparent density and relative density of the $(Ba_{1-x}Sr_x)_4(Sm_{0.4}Nd_{0.6})_{28/3}Ti_{18}O_{54}$ $(0.02 \leqslant x \leqslant 0.1)$ ceramics. As can be seen from Fig. 6(a), the increasing Sr^{2+} content causes a reduction of the apparent density of the ceramics. At the same time, from Fig. 6(b), it is found that apparent density and relative density of the $(Ba_{1-x}Sr_x)_4(Sm_{0.4}Nd_{0.6})_{28/3}Ti_{18}O_{54}$ ($x = 0.08$) ceramic gradually increase with the increase of sintering temperature and then obviously decrease at the further sintering temperature. Furthermore, the apparent density of $(Ba_{1-x}Sr_x)_4(Sm_{0.4}Nd_{0.6})_{28/3}Ti_{18}O_{54}$ ($x = 0.08$) ceramic reaches the maximum value at 1440 ℃ for 4 h. The larger apparent density means the less crystal imperfection and porosity in the sample's interior structure, and a higher $Q \times f$ value will be obtained.

3.3 Dielectric properties

Figure 7(a) shows the variation of the $Q \times f$ value and permittivity (ε_r) of $(Ba_{1-x}Sr_x)_4(Sm_{0.4}Nd_{0.6})_{28/3}Ti_{18}O_{54}$ ceramics sintered at 1400 ℃ for 4 h. According to the literature [29], the $Q \times f$ value and permittivity (ε_r) of $Ba_{6-3y}(Sm_{0.4}Nd_{0.6})_{8+2y}Ti_{18}O_{54}$ ($y = 2/3$) ceramic is ~10,700 GHz and ~82.7, respectively. As shown in Fig. 7(a), after adding Sr^{2+} ions into the system, the permittivity (ε_r) firstly increases from 90.82 to 93.19 while x value varies from 0.02 to 0.08, and then the permittivity (ε_r) decreases to 89.76 at $x = 0.1$. This improvement may be caused by the relaxation of local

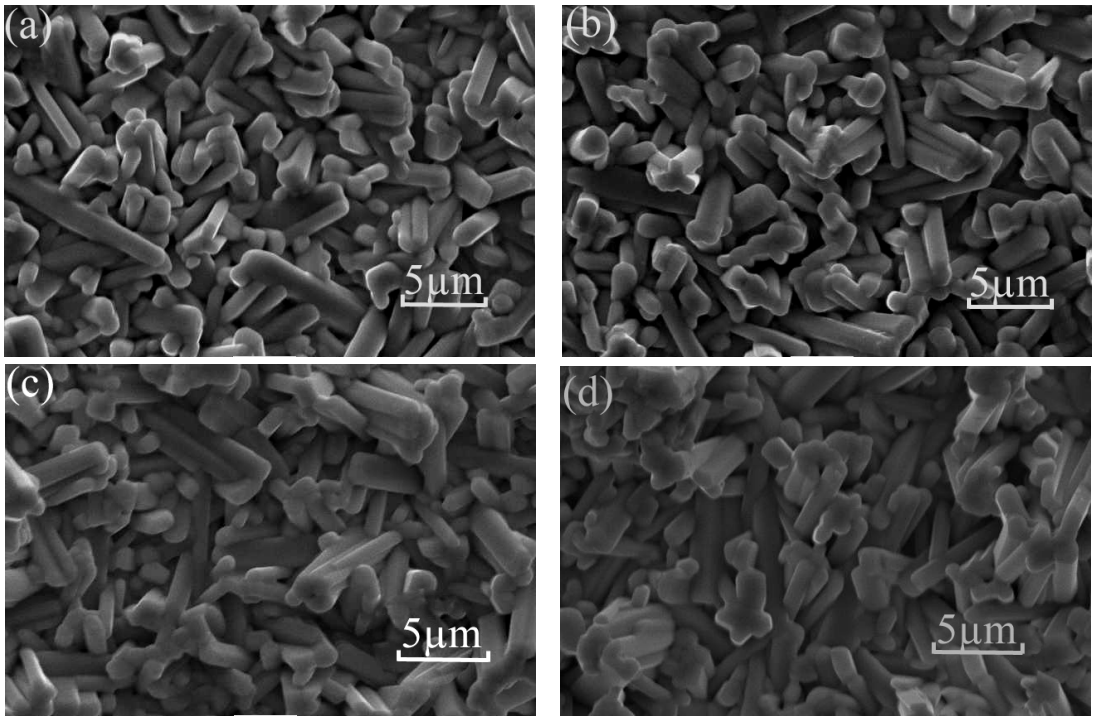

Fig. 5 SEM micrographs of $(Ba_{1-x}Sr_x)_4(Sm_{0.4}Nd_{0.6})_{28/3}Ti_{18}O_{54}$ ceramic for $x=0.08$ sintered at various temperatures with (a) 1400 ℃, (b) 1420 ℃, (c) 1440 ℃, (d) 1460 ℃.

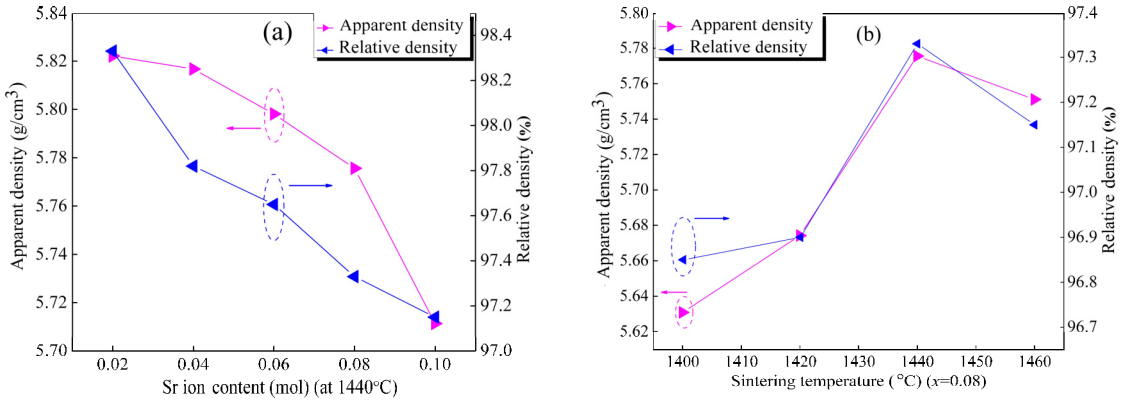

Fig. 6 (a) Influence of the apparent density and relative density of the $(Ba_{1-x}Sr_x)_4(Sm_{0.4}Nd_{0.6})_{28/3}Ti_{18}O_{54}$ ceramics on the amount of Sr^{2+} ions; (b) influence of the apparent density and relative density of the $(Ba_{1-x}Sr_x)_4(Sm_{0.4}Nd_{0.6})_{28/3}Ti_{18}O_{54}$ ($x=0.08$) ceramic at different sintering temperatures.

distortions at A2 sites, which results from the substitution of smaller Sr^{2+} ions for Ba^{2+} ions [30]. Meanwhile, the corresponding $Q\times f$ value slightly decreases from 10264 to 9200 GHz while x varies from 0.02 to 0.1. The dielectric relaxation caused by its large resistivity is one of the reason for the dielectric loss of $(Ba_{1-x}Sr_x)_4(Sm_{0.4}Nd_{0.6})_{28/3}Ti_{18}O_{54}$ ceramics [31–33]. Herein, the optimal microwave dielectric properties of $\varepsilon_r\approx93.19$, $Q\times f\approx9770.14$ GHz (at 3.415 GHz) can be achieved at $x=0.08$. The uprising of permittivity (ε_r) with x value should be attributed to the presence of Sr^{2+} ions substituted for Ba^{2+} ions and the coexistence of $BaSm_2Ti_4O_{12}$ and $BaNd_2Ti_5O_{14}$ phases. In addition, the $Q\times f$ value and ε_r of the $(Ba_{1-x}Sr_x)_4(Sm_{0.4}Nd_{0.6})_{28/3}Ti_{18}O_{54}$ ceramic for $x=0.08$ as a function of its sintering temperature for 4 h are shown in Fig. 7(b). In Fig. 7(b), the $Q\times f$ value of the $(Ba_{1-x}Sr_x)_4(Sm_{0.4}Nd_{0.6})_{28/3}Ti_{18}O_{54}$ ceramic for $x=0.08$ sintered at 1440 ℃ is relatively high due to the high density and the compact microstructure. With an increasing of sintering temperature, the $Q\times f$ value of the $(Ba_{1-x}Sr_x)_4(Sm_{0.4}Nd_{0.6})_{28/3}Ti_{18}O_{54}$ ceramic for $x=0.08$ increases to a maximum value of 9770.14 GHz (at 3.415 GHz) and decreases thereafter.

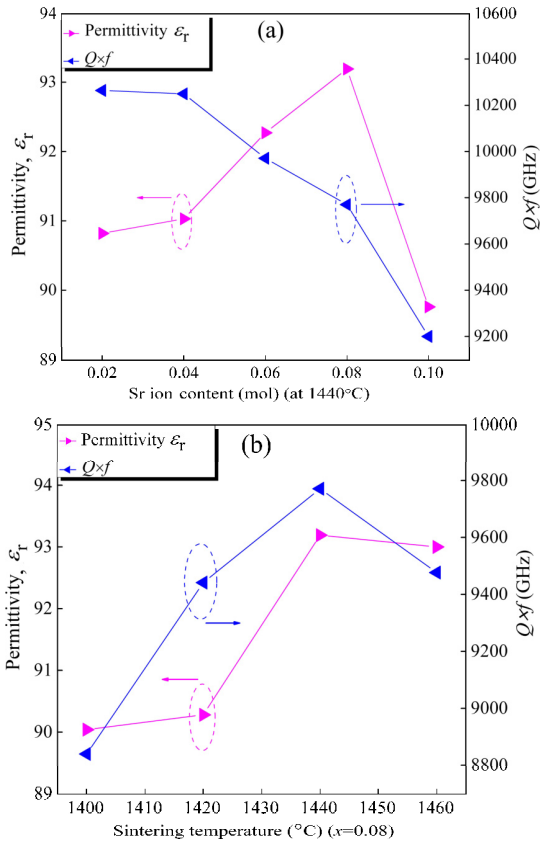

Fig. 7 (a) Influence of the $Q\times f$ value and dielectric constant (ε_r) of the $(Ba_{1-x}Sr_x)_4(Sm_{0.4}Nd_{0.6})_{28/3}Ti_{18}O_{54}$ ceramics on the amount of Sr^{2+} ions; (b) influence of the $Q\times f$ value and dielectric constant (ε_r) of the $(Ba_{1-x}Sr_x)_4(Sm_{0.4}Nd_{0.6})_{28/3}Ti_{18}O_{54}$ ($x=0.08$) ceramic at different sintering temperatures.

Figure 8 shows the variation of τ_f, electronegativity (e), and tolerance factor (t) of the $(Ba_{1-x}Sr_x)_4(Sm_{0.4}Nd_{0.6})_{28/3}Ti_{18}O_{54}$ ($0.02 \leqslant x \leqslant 0.1$) ceramics sintered at 1440 ℃ for 4 h. In Fig. 8, it is noted that the changes of τ_f, electronegativity (e), and tolerance factor (t) show the same trend with the increase of x value, and the minimum values of all the parameters can be obtained at $x=0.1$, which indicates that the changes of τ_f are mainly dependent on the electronegativity (e) and tolerance factor (t) of the $(Ba_{1-x}Sr_x)_4(Sm_{0.4}Nd_{0.6})_{28/3}Ti_{18}O_{54}$ ceramics. Therefore, the value of τ_f can be adjusted by Sr^{2+} ion addition with changing in the tolerance factor (t). Wherein, the tolerance factor can be calculated by the following equation:

$$t=\frac{\frac{14}{15}(0.4R_{Sm^{3+}}+0.6R_{Nd^{3+}})+\frac{1}{15}[(1-x)R_{Ba^{2+}}+xR_{Sr^{2+}}]+R_{O^{2-}}}{\sqrt{2}(R_{Ti^{4+}}+R_{O^{2-}})} \quad (3)$$

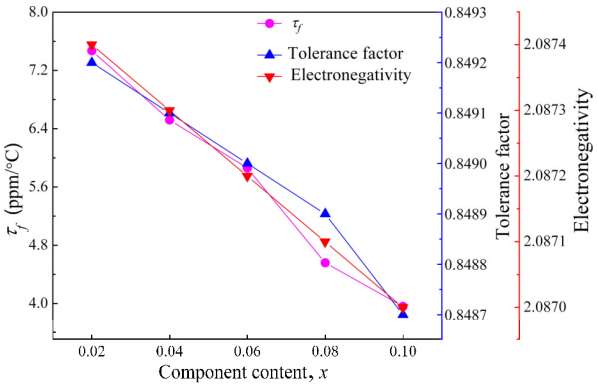

Fig. 8 Variation of the temperature coefficient of resonant frequency (τ_f), electronegativity (e), and tolerance factor (t) of the $(Ba_{1-x}Sr_x)_4(Sm_{0.4}Nd_{0.6})_{28/3}Ti_{18}O_{54}$ ceramics with different x values sintered at 1440 ℃ for 4 h.

where $R_{Sm^{3+}}$, $R_{Nd^{3+}}$, $R_{Ba^{2+}}$, $R_{Sr^{2+}}$, $R_{Ti^{4+}}$, and $R_{O^{2-}}$ represent the ionic radii of Sm^{3+}, Nd^{3+}, Ba^{2+}, Sr^{2+}, Ti^{4+}, and O^{2-}, respectively [34,35]. In addition, the reduction of t illustrates that the symmetry in $BaNd_2Ti_5O_{14}$ phase has a reduction in the increase of x value. With the increase of the Sr^{2+} ion content, the electronegativity of the tungsten bronze structure almost decreases linearly. Meanwhile, the changes of τ_f are almost consistent with the variation of electronegativity, which also shows that the τ_f values are strongly related with the electronegativity in tungsten bronze structure. Wherein, the electronegativity (e) of the $(Ba_{1-x}Sr_x)_4(Sm_{0.4}Nd_{0.6})_{28/3}Ti_{18}O_{54}$ solid solution can be calculated by the following equation:

$$e=\frac{4[(1-x)X_{Ba\text{-}O}+xX_{Sr\text{-}O}]+\frac{28}{3}(0.4X_{Sm\text{-}O}+0.6X_{Nd\text{-}O})+18X_{Ti\text{-}O}}{32-\frac{2}{3}} \quad (4)$$

where $X_{Ba\text{-}O}$, $X_{Sr\text{-}O}$, $X_{Sm\text{-}O}$, $X_{Nd\text{-}O}$, and $X_{Ti\text{-}O}$ represent the electronegativity difference of Ba^{2+}, Sr^{2+}, Sm^{3+}, Nd^{3+}, and Ti^{4+} with O^{2-}, respectively [36].

4 Conclusions

$(Ba_{1-x}Sr_x)_4(Sm_{0.4}Nd_{0.6})_{28/3}Ti_{18}O_{54}$ ($x=0.02$, 0.04, 0.06, 0.08, 0.1) ceramics were prepared by the conventional solid-state reaction method and well densified at ~1440 ℃. The phase structures, grain morphologies, and microwave dielectric properties of the $(Ba_{1-x}Sr_x)_4(Sm_{0.4}Nd_{0.6})_{28/3}Ti_{18}O_{54}$ ceramics were studied. The phase structures and microwave dielectric properties were greatly influenced by x value. The optimal

microwave dielectric properties with a permittivity (ε_r) ≈ 93.19, a quality factor ($Q \times f$) ≈ 9770.14 GHz (at 3.415 GHz), and an almost near-zero temperature coefficient of resonant frequency (τ_f) ≈ +4.56 ppm/℃ can be obtained for the $(Ba_{0.92}Sr_{0.08})_4(Sm_{0.4}Nd_{0.6})_{28/3}Ti_{18}O_{54}$ specimen sintered at 1440 ℃ for 4 h. Also, these results indicated that the $(Ba_{0.92}Sr_{0.08})_4(Sm_{0.4}Nd_{0.6})_{28/3}Ti_{18}O_{54}$ ceramic with very high permittivity (ε_r), high quality factor ($Q \times f$), and almost near-zero temperature coefficient of resonant frequency (τ_f) is a suitable candidate for microwave passive component applications.

Acknowledgements

Financial supports of the National Natural Science Foundation of China (Grant No. 11464006) and the Middle-aged and Young Teachers in Colleges and/or Universities in Guangxi Basic Ability Promotion Project of China (Grant No. KY2016YB534) are gratefully acknowledged by the authors.

References

[1] Wersing W. Microwave ceramics for resonators and filters. *Current Opinion in Solid State and Materials Science* 1996, **1**: 715–731.

[2] Bolton RL. Temperature compensating ceramic capacitors in the system barium-rare earth oxide titania. Ph.D. Thesis. The University of Illinois, 1968.

[3] Sremoolanathan H, Sebastian MT, Pezholil M. Dielectric resonators in $BaO–Ln_2O_3–5TiO_2$ system (Ln = La, Pr, Nd, Sm). *British Ceramic Transactions* 1996, **95**: 79–81.

[4] Ohsato H. Science of tungstenbronze-type like $Ba_{6-3x}R_{8+2x}Ti_{18}O_{54}$ (R = rare earth) microwave dielectric solid solutions. *J Eur Ceram Soc* 2001, **21**: 2703–2711.

[5] Valant M, Suvorov D, Rawn CJ. Intrinsic reasons for variations in dielectric properties of $Ba_{6-3x}R_{8+2x}Ti_{18}O_{54}$ (R = LA–Gd) solid solutions. *Jpn J Appl Phys* 1999, **38**: 2820.

[6] Varfolomeeva MB, Miranov AS. The synthesis and homogeneity ranges of the phases $Ba_{6-3x}Ln_{8+2x}Ti_{18}O_{54}$. *Russ J Inorg Chem* 1988, **33**: 607.

[7] Kolar D, Skapin SD, Suvorov D. Phase equlibria in the system $BaO–TiO_2–Gd_2O_3$. *Acta Chimica Slovenica* 1999, **46**: 193–202.

[8] Kolar D, Gaberščček S, Stadler Z, *et al*. High stability, low loss dielectrics in the system $BaO–Nd_2O_3–TiO_2–Bi_2O_3$. *Ferroelectrics* 1980, **27**: 269–272.

[9] Ohsato H, Ohhashi T, Kato H, *et al*. Microwave dielectric properties and structure of the $Ba_{6-3x}Sm_{8+2x}Ti_{18}O_{54}$ solid solutions. *Jpn J Appl Phys* 1995, **34**: 187–191.

[10] Yao X, Lin H, Zhao X, *et al*. Effects of Al_2O_3 addition on the microstructure and microwave dielectric properties of $Ba_4Nd_{9.33}Ti_{18}O_{54}$ ceramics. *Ceram Int* 2012, **38**: 6723–6728.

[11] Ohsato H, Mizuta M, Ikoma T, *et al*. Microwave dielectric properties of tungsten bronze-type $Ba_{6-3x}R_{8+2x}Ti_{18}O_{54}$ (R = La, Pr, Nd and Sm) solid solutions. *J Ceram Soc Jpn* 1998, **106**: 178–182.

[12] Pei J, Yue Z, Zhao F, *et al*. Effects of silver doping on the sol–gel-derived $Ba_4(Nd_{0.7}Sm_{0.3})_{9.33}Ti_{18}O_{54}$ microwave dielectric ceramics. *J Am Ceram Soc* 2007, **90**: 3131–3137.

[13] Ubic R, Reaney IM, Lee WE, *et al*. Properties of the microwave dielectric phase $Ba_{6-3x}Nd_{8+2x}Ti_{18}O_{54}$. *Ferroelectrics* 1999, **228**: 271–282.

[14] Huang X, Zhang J, Wang W, *et al*. Effect of pH value on electromagnetic loss properties of Co–Zn ferrite prepared via coprecipitation method. *J Magn Magn Mater* 2016, **405**: 36–41.

[15] Huang X, Zhang J, Xiao S, *et al*. Unique electromagnetic properties of the zinc ferrite nanofiber. *Mater Lett* 2014, **124**: 126–128.

[16] Sebastian MT. *Dielectric Materials for Wireless Communication*. Elsevier, 2010.

[17] Nagatomo T, Otagiri T, Suzuki M, *et al*. Microwave dielectric properties and crystal structure of the tungstenbronze-type like $(Ba_{1-\alpha}Sr_\alpha)_6(Nd_{1-\beta}Y_\beta)_8Ti_{18}O_{54}$ solid solutions. *J Eur Ceram Soc* 2006, **26**: 1895–1898.

[18] Zhu J, Kipkoech ER, Lu W. Effects of $LnAlO_3$ (Ln = La, Nd, Sm) additives on the properties of $Ba_{4.2}Nd_{9.2}Ti_{18}O_{54}$ ceramics. *J Eur Ceram Soc* 2006, **26**: 2027–2030.

[19] Zheng H, Reaney IM, Muir D, *et al*. Effect of glass additions on the sintering and microwave properties of composite dielectric ceramics based on $BaO–Ln_2O_3–TiO_2$ (Ln = Nd, La). *J Eur Ceram Soc* 2007, **27**: 4479–4487.

[20] Jacob KS, Satheesh R, Ratheesh R. Preparation and microwave characterization of $BaNd_{2-x}Sm_xTi_4O_{12}$ ($0 \leqslant x \leqslant 2$) ceramics and their effect on the temperature coefficient of dielectric constant in polytetrafluoroethylene composites. *Mater Res Bull* 2009, **44**: 2022–2026.

[21] Xia H-T, Kuang X-J, Wang C-H, *et al*. Conductivity and dielectric loss of tungsten-bronze-type $BaNd_2Ti_4O_{12}$ microwave ceramics. *Acta Phys-Chim Sin* 2011, **27**: 2009–2014.

[22] Wu M-C, Hsieh M-K, Yen C-W, *et al*. Low sintering $BaNd_2Ti_4O_{12}$ microwave ceramics prepared by CuO thin layer coated powder. *J Eur Ceram Soc* 2007, **27**: 2835–2839.

[23] Long M, Zhuang W, Tang B, *et al*. Microwave dielectric properties of $Ba_{0.75}Sr_{0.25}(Nd_xBi_{1-x})_2Ti_4O_{12}$ solid solutions. *Ceram–Silikáty* 2011, **55**: 373–377.

[24] Long M, Zhuang W, Tang B, *et al*. Effect of molar ratio of Nd/Bi on the microwave ceramic properties of $Ba_{0.75}Sr_{0.25}(Nd_xBi_{1-x})_2Ti_4O_{12}$ microwave materials. *Piezoelectrics & Acoustooptics* 2012, **34**: 106–109. (in Chinese)

[25] Zhang Y-D, Zhou D, Guo J, *et al*. Microwave dielectric properties of the $(1–x)(Mg_{0.95}Zn_{0.05})TiO_3–x(Ca_{0.8}Sm_{0.4/3})TiO_3$ temperature stable ceramics. *Mater Lett* 2014, **32**: 200–202.

[26] Pang L-X, Zhou D, Cai C-L, *et al*. Infrared spectroscopy

and microwave dielectric properties of ultra-low temperature firing $(K_{0.5}La_{0.5})MoO_4$ ceramics. *Mater Lett* 2013, **92**: 36–38.

[27] Zhou H, Liu X, Chen X, *et al*. $Ba_4LiNb_{3-x}Sb_xO_{12}$: Phase evolution, microstructure and optimized microwave dielectric properties. *Mater Lett* 2013, **96**: 199–202.

[28] Wang X, Fu R, Chen X. Crystal structure and microwave dielectric properties of $(Ba_{1-\alpha}Sr_\alpha)Sm_2Ti_4O_{12}$ solid solutions. *J Mater Sci: Mater El* 2016, **27**: 11137–11141.

[29] Webhoffer A, Feltz A. Microwave dielectric properties of ceramics of the system $Ba_{6-x}(Sm_yNd_{1-y})_{8+2x/3}Ti_{18}O_{54}$. *J Mater Sci Lett* 1999, **18**: 719–721.

[30] Kagomiya I, Suzuki M, Kakimoto K, *et al*. Microwave dielectric properties of tungsten bronze type like $(Ba_{1-\alpha}Sr_\alpha)_{6-3x}R_{8+2x}Ti_{18}O_{54}$ (R = Sm, Nd) solid solutions. *J Eur Ceram Soc* 2007, **27**: 3059–3062.

[31] Huang X, Chen Y, Yu J, *et al*. Fabrication and electromagnetic loss properties of Fe_3O_4 nanofibers. *J Mater Sci: Mater El* 2015, **26**: 3474–3478.

[32] Huang X, Zhang J, Liu Z, *et al*. Facile preparation and microwave absorption properties of porous hollow $BaFe_{12}O_{19}/CoFe_2O_4$ composite microrods. *J Alloys Compd* 2015, **648**: 1072–1075.

[33] Melvin GJH, Ni Q-Q, Natsuki T. Electromagnetic wave absorption properties of barium titanate/carbon nanotube hybrid nanocomposites. *J Alloys Compd* 2014, **615**: 84–90.

[34] Zheng XH, Chen XM. Dielectric ceramics with tungsten bronze structure in $BaO–Nd_2O_3–TiO_2–Nb_2O_5$ system. *J Mater Res* 2002, **17**: 1664–1670.

[35] Shannon RD. Revised effective ionic radii and systematic studies of interatomic distances in halides and chalcogenides. *Acta Cryst* 1976, **A32**: 751–767.

[36] Chen XM, Li Y. A- and B site cosubstituted $Ba_{6-3x}Sm_{8+2x}Ti_{18}O_{54}$ microwave dielectric ceramics. *J Am Ceram Soc* 2002, **85**: 579–584.